



Highly efficient removal of toxic ions by the activated carbon derived from *Citrus limon* tree leaves

Fahime Nemati¹ · Dariush Jafari² · Hossein Esmaeili²

Received: 22 February 2020 / Revised: 21 July 2020 / Accepted: 28 August 2020 / Published online: 4 September 2020
© Korean Carbon Society 2020

Abstract

The purpose of this study was to remove lead and arsenic ions from aqueous solutions using the activated carbon prepared from *Citrus limon* tree leaves. Characteristics of the prepared adsorbent were studied thoroughly using BET, SEM, EDS and mapping, XRD, and RAMAN analyses. The results of experiments showed that the highest adsorption efficiencies were 97.67% and 95.89% for Pb (II) and As (III), respectively. Additionally, the adsorbent was successfully regenerated four times and therefore it was able to perform the adsorption and desorption processes well. Moreover, the results of adsorption kinetics showed that the pseudo second-order kinetic model was more effective for the description of adsorption mechanism of both metals. Furthermore, the equilibrium studies indicated that Langmuir and Freundlich isotherm models were desirable for lead and arsenic ions, respectively.

Keywords Activated carbon adsorbent · *Citrus limon* tree · Adsorption · Aqueous solution · Lead · Arsenic

1 Introduction

Environmental pollution is now considered as a critical global issue [1]. As a result of population explosion and the development of industries and agriculture in recent years, besides the lack of clean water resources, accessibility to clean water and its recycle has become a worldwide necessity. Heavy metals are the pollutants which are naturally produced from industrial processes and human activities [2, 3]. Due to the extent, durability, and toxicity of these contaminants in aqueous solutions, metallic ions have been reported as severe harmful chemicals to the human life and environment [4–6]. Such metals can pollute water sources and food chain and also enter the human body through

various ways, including drinking water, food, and breathing the suspended particles [7]. Some of heavy metals such as lead, cadmium, mercury, arsenic, and nickel are toxic at even very low traces [8, 9]. The main source of environment pollution by heavy metals is the wastewater of industries like electroplating, metallurgy, and production of electric boards. The annual direct discharge of wastewater of such industries without any specific treatment into the environment causes a deadly risk of human health. There are several methods for the removal of these heavy metals from wastewaters including filtration, reverse osmosis, ion exchange resin, chemical treatment, and adsorption [10, 11]. Among the mentioned treatment methods, due to its environmental compatibility, simplicity, high separation efficiency, and being technically feasible [12, 13], adsorption has received considerable critical attention [14, 15]. Various adsorbents have been used to remove heavy metals from wastewater systems so far, among them the activated carbon is one of the most important types [16–18]. In recent years, the use of bio-activated carbon has been a major area of interest for its environmental compatibility and very high removal efficiency [19].

In the present work, the activated carbon which was prepared from *Citrus limon* tree leaves was used as a novel and effective adsorbent to remove Pb (II) and As (III) ions from aqueous solutions. To do so, various parameters such as solution pH, adsorbent dosage, concentration of lead and

✉ Dariush Jafari
dariush.jafari@yahoo.com

Fahime Nemati
fahime.nemati10@gmail.com

Hossein Esmaeili
esmaeili.hossein@gmail.com

¹ Department of Chemical Engineering, School of Chemical Engineering, Kherad Institute of Higher Education, Bushehr, Iran

² Department of Chemical Engineering, Bushehr Branch, Islamic Azad University, Bushehr, Iran

arsenic metallic ions, contact time, and temperature were investigated and the maximum removal efficiencies of lead and arsenic ions were obtained. Additionally, kinetic, equilibrium, and thermodynamic studies of the adsorption process were investigated. It should be noted that the adsorbent was regenerated and reused. To our knowledge, there is not any paper available in the literature that has discussed the usage of such an adsorbent for the removal of lead and arsenic ions.

2 Materials and methods

2.1 Chemicals

The leaves of *Citrus limon* tree, which were used in the current study as a source for the preparation of activated carbon, were collected from local gardens of Boushehr province (Iran). Sodium hydroxide, hydrochloric acid, lead nitrate ($\text{Pb}(\text{NO}_3)_2$), and sodium arsenite (NaAsO_2) were all purchased from Merck Company (Germany) with a purity of > 99%. Their chemical formula, CAS registry number, suppliers, and chemical structure are presented in Table 1. It should be noted that double distilled water was used in all of the experiments to prepare lead and arsenic ions solutions.

2.2 Preparation of stock solution

To prepare the stock solutions of lead and arsenic ions with an initial concentration of 1000 ppm, 1.6 g of $\text{Pb}(\text{NO}_3)_2$ and 1.73 g of NaAsO_2 were accurately weighted and poured into a 250 ml volumetric flask and dissolved in double distilled water. Stock solutions with lower concentrations were then prepared by dilution using double distilled water.

2.3 Preparation of adsorbent

For the preparation of the activated carbon adsorbent, the collected *Citrus limon* tree leaves were washed by water to

remove any residual dust and other impurities. After washing, the *Citrus limon* tree leaves were dried completely in an oven for 2 h in temperature of 100 °C. Then, the dried leaves were placed in an inert gas furnace for 4 h in temperature of 700 °C. After the aforementioned period of time, the carbonized materials were graded using sieve no. 25 and held in polyethylene sealed containers in ambient temperature for further use as the adsorbent.

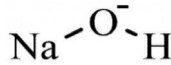
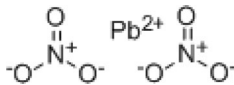
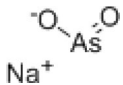
When the activated carbon adsorbent was prepared, its surface and structural properties were determined using various analyses. Techniques such as BET (Belsorp, Belsorp mini II, Japan), SEM (Tisteam MIRA III, Czech Republic), Energy-dispersive X-ray spectroscopy (EDS) and Mapping (Map) (Tisteam SAM x, France), XRD (X-Pert-PrompD Panalytical, The Netherland), and RAMAN (Takram p50C0R10 Iran) were applied to determine the adsorbent specific surface area, its structure and morphology, the elements and their weight percentages on the adsorbent structure, and the adsorbent crystallinity.

2.4 Experimental procedure

As mentioned before, lead and arsenic ions adsorption experiments were carried out in a 250 ml volumetric flask containing 100 ml of these ions solutions using the activated carbon prepared from *Citrus limon* tree leaves. For this purpose, the effect of different parameters such as pH (2–11), adsorbent dosage (0.25–10 g/L), initial concentration of metallic ions (10–100 mg/L), contact time (5–180 min), and temperature (25–55 °C) were investigated on their adsorption efficiencies. After the tests and separation of adsorbent from aqueous solution, an atomic absorption spectrometry equipped with acetylene-air fuel (VARIAN, USA) was used to determine the amount of remaining ions in the aqueous solution.

To determine the adsorption efficiency of metallic ions from the aqueous solutions, Eq. (1) was used:

Table 1 The chemical formula, CAS registry number, suppliers, and chemical structure of the chemicals

Compound	Chemical formula	CAS registry number	Suppliers	2D schematic of chemical structure
Sodium hydroxide	NaOH	1310-73-2	Merck Co., Germany	
Hydrochloric acid	HCl	7647-01-0	Merck Co., Germany	$\text{H}^+\text{-Cl}^-$
Lead (II) nitrate	$\text{Pb}(\text{NO}_3)_2$	10,099-74-8	Merck Co., Germany	
Sodium arsenite	NaAsO_2	7784-46-5	Merck Co., Germany	

$$\text{Re} (\%) = \frac{C_i - C_{oe}}{C_i} \times 100, \quad (1)$$

where Re is the percentage of the ion's removal, and C_i and C_e (mg/L) are the initial and equilibrium concentrations of the metallic ion in aqueous solution, respectively. In addition, the adsorption equilibrium capacity per gram of the dry adsorbent was determined from Eq. (2):

$$q_e = \frac{(C_i - C_e)}{w} \times V. \quad (2)$$

In this equation, q_e is the adsorption capacity (mg/g), V is the volume of solution (L), and W is the mass of the used adsorbent (g).

3 Results and discussion

3.1 Adsorbent characterizations

BET analysis was used to study the surface properties of the prepared activated carbon. The results showed that the specific surface area, pore volume, and average diameter of the adsorbent cavities were 291.93 m²/g, 425.95 cm³/g, and 5.83 nm, respectively. According to these data, the adsorbent has an acceptable specific surface area which makes it suitable for adsorbing the metal ions. Additionally, the diameter of the cavities represents the mesoporous nature of the adsorbent.

SEM analysis was applied to determine the morphology of the activated carbon adsorbent before and after adsorption of lead and arsenic ions. As it can be observed in Fig. 1, the adsorbent has a rough structure with high number of adsorption channels before the adsorption process, while its surface became uniform after the adsorption of ions and

the adsorption sites disappeared because they were occupied by the adsorbed metallic ions. The surface uniformity and disappearance of adsorption sites are clearly shown in Fig. 1b, c.

EDS and MAP analyses were used to investigate the distribution of the existing elements on the adsorbent surface which confirms its ability to adsorb lead and arsenic ions. The results of EDS and MAP analyses are shown in Fig. 2 and Table 2, respectively. As reported in this table, there are several elements on the surface of activated carbon and the highest weight percentages belong to carbon and oxygen which were 22.6% and 33.7%, respectively. After the adsorption of Pb and As ions, EDS and MAP analyses confirmed the presence of these elements on the adsorbent structure, which indicates that the applied adsorbent was capable of adsorbing them. It should be noted that the weight percentages of lead and arsenic elements on the activated carbon structure after the adsorption process were 37.39% and 0.73%, respectively, indicating the higher adsorption capability of the prepared activated carbon for lead ions. Moreover, the results of Ultimate analysis of the dry leaves are presented in this table. It is clearly seen that the composition of C and O elements are much higher than others.

XRD analysis was applied to determine the type of the adsorbent's crystalline phases and its crystallinity. XRD spectrum of the current adsorbent before and after adsorption of lead and arsenic ions are shown in Fig. 3. As it can be observed, there are some peaks in 2θ values around 23°, 31°, and 43°, which can be associated with (002) and (001) crystalline phases of the graphite structure [20]. Actually, the peak in $2\theta = 43^\circ$ is associated with (100) and (101) crystalline phase, which confirms the graphite structure of the current prepared activated carbon [21, 22]. According to the presented XRD spectrum, the peaks of the CaCO₃, KCl, CaSO₄, Ca₃(PO₄)₂ and MgO/67H₂O compounds match with the reference

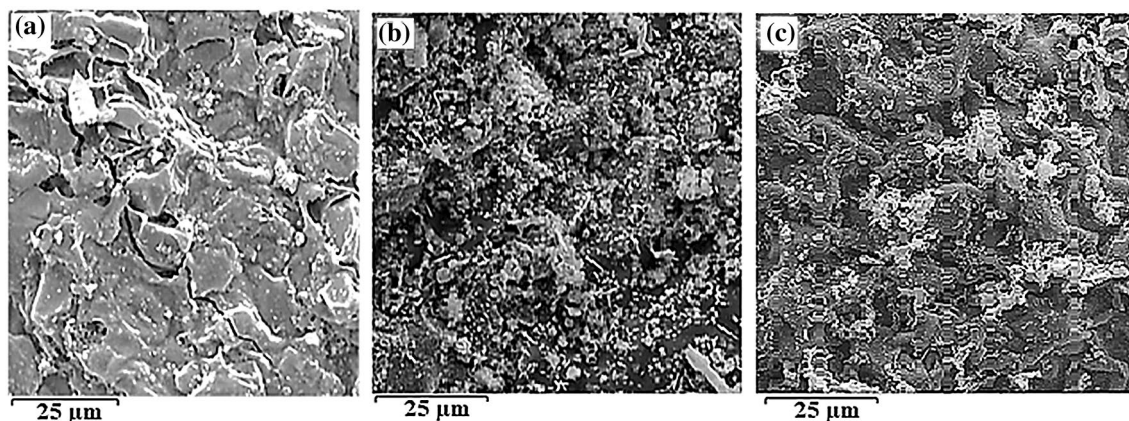


Fig. 1 SEM images of activated carbon adsorbent prepared from *Citrus limon* tree leaves (a) before the adsorption, b after the adsorption of lead ions, and c after the adsorption of arsenic ions

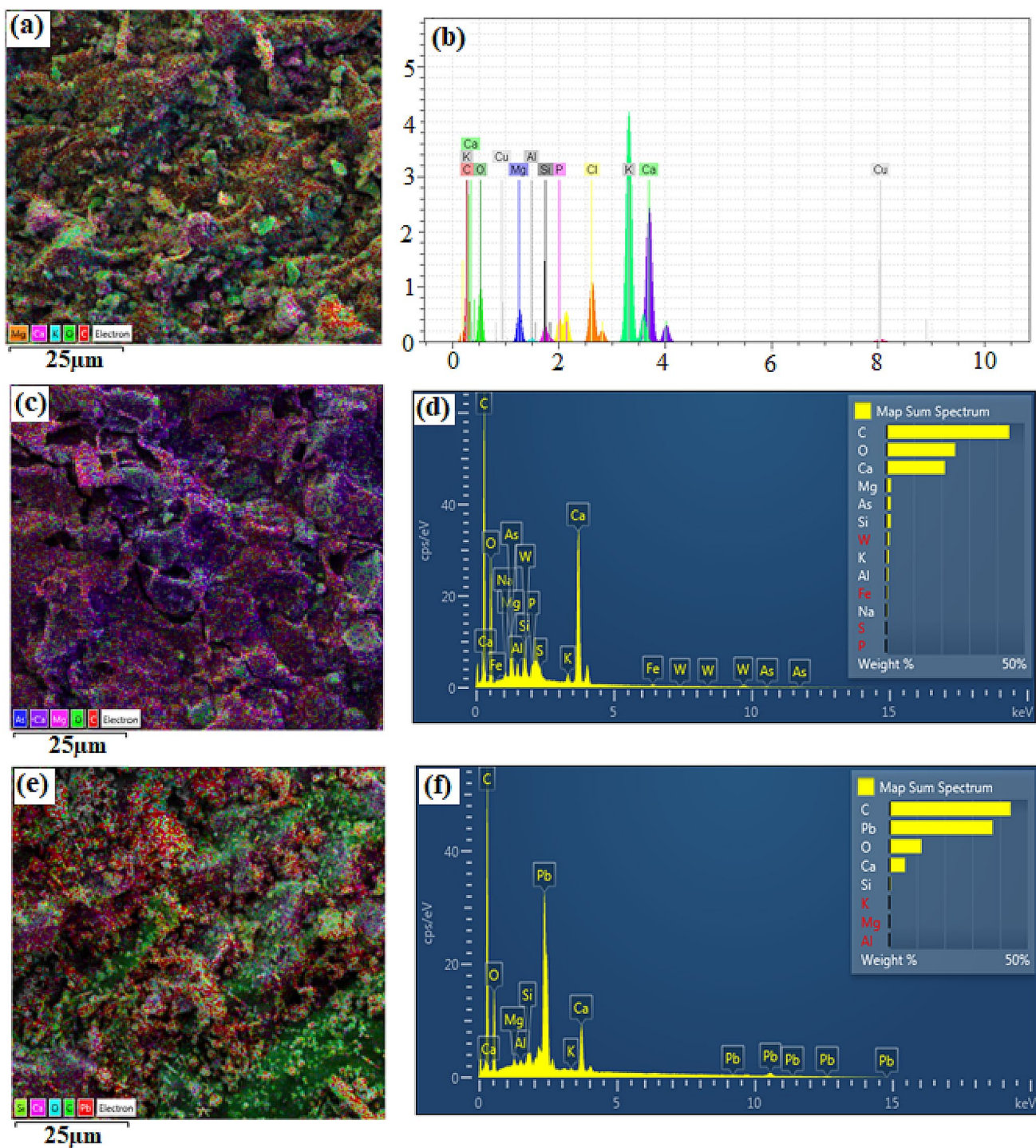


Fig. 2 EDS and Map analyses for (a, b) activated carbon adsorbent, (c, d) after the adsorption of arsenic ions, (e, f) and after the adsorption of lead ions

card numbers of 24-0027, 41-1476, 36-0617, 32-0176, and 11-0353, respectively. The maximum peaks revealed in 2θ values of 29.5, 28.5, 25.5, and 14.5 are the characteristics of CaCO_3 , KCl , $\text{Ca}_3(\text{PO}_4)_2$, and CaSO_4 structure, respectively. Considering Fig. 3b and c, the location and

intensity of the observed peaks were not changed considerably after the adsorption of the metallic ions, therefore it can be concluded that the activated carbon's crystalline structure was unchanged by the adsorption of the ions.

Table 2 Weight percentages of dry leaves and activated carbon constituents prepared from *Citrus limon* tree leaves before and after the lead and arsenic metal ions adsorption processes from the aqueous solution

Element (wt%)	Ultimate analysis data (dry leaves)	Activated carbon	Adsorbent after adsorption As (III)	Adsorbent after adsorption Pb (II)
C	49.61	22.60	44.45	43.89
O	38.23	33.70	24.97	11.62
Na	–	–	0.43	–
Mg	–	2.18	1.80	0.29
Al	–	0.24	0.81	9.23
Si	–	1.01	1.72	0.51
P	–	3.01	–	–
S	2.17	–	0.03	–
Cl	–	4.29	–	–
K	–	18.83	1.00	0.29
Ca	–	13.16	21.21	5.78
Fe	–	–	0.65	–
Cu	–	0.99	–	–
Ta	–	–	–	–
As	–	–	0.73	–
Pb	–	–	–	37.39
N	3.21	–	–	–
H	6.78	–	–	–
Total	100	100.00	100.00	100.00

RAMAN spectroscopy is one of the techniques which can be used to describe various functional groups, the degree of quantum change [23], as well as the structural study of the materials [24]. It is worth noting that this analysis is highly sensitive to the amorphous bonds in the structure of material [23]. The results of RAMAN analysis for the current activated carbon before and after the adsorption of lead and arsenic ions are shown in Fig. 4. The main characteristics of the resulting spectra are two peaks called D and G peaks. The G peak which is located in the range of 1586 cm^{-1} is associated with the E_{2g} vibration mode and represents the SP^2 hybrid structure of the carbon, indicating the crystalline nature of the prepared adsorbent. In addition, the D peak which is appeared in the range of 1371 cm^{-1} indicates the hybrid SP^3 structure of carbon [25] and the amorphous section of the prepared adsorbent. It is also worth noting that the intensity and width of the G and D peaks present some information about the disturbances in the adsorbent sample. The D/G ratio intensity for the produced activated carbon before and after adsorption of arsenic and lead ions were 0.858, 0.848, and 0.857, respectively. The decrease in this ratio shows that after the process, the amount of crystalline portions in the activated carbon increased similar to its hybrid SP^2 structure, which could be due to adsorption of lead and arsenic metal ions [25]. It should be noted that RAMAN spectrum of the prepared activated carbon was changed after the adsorption of lead and arsenic ions. The current findings mirror those of the previous studies [26].

Therefore, according to the obtained results, it can be stated that activated carbon has both amorphous and crystalline portions, and the adsorption of lead and arsenic heavy metals ions increased the crystalline portions of the produced adsorbent's structure.

3.2 Effect of solution pH

pH is a key factor of the adsorption process, since it affects the surface charge of the adsorbent. The effect of pH on the adsorption efficiencies of lead and arsenic ions was studied in the range of 2–11, and the results are shown in Fig. 5. As can be seen in this figure, by increasing pH, the removal efficiencies of lead and arsenic ions increase to a maximum point. The highest adsorption efficiencies were achieved for lead (96.82%) and arsenic (95.98%) in pH values of 7 and 9, respectively. This can be described according to the anion characteristics of *Citrus limon* tree leaves. Additionally, at lower pH values ($\text{pH} < 5$), the removal efficiencies of lead and arsenic were low, which indicate that acidic pH is not suitable for the removal of these two metals. These initial increases in the adsorption efficiency values are due to the presence of negative charges on the adsorbent's surface, which can be considered as the proper location of the metal ion adsorption sites. However, in low pH values, the hydrogen ions (H^+) present in the aqueous phase compete with the metallic

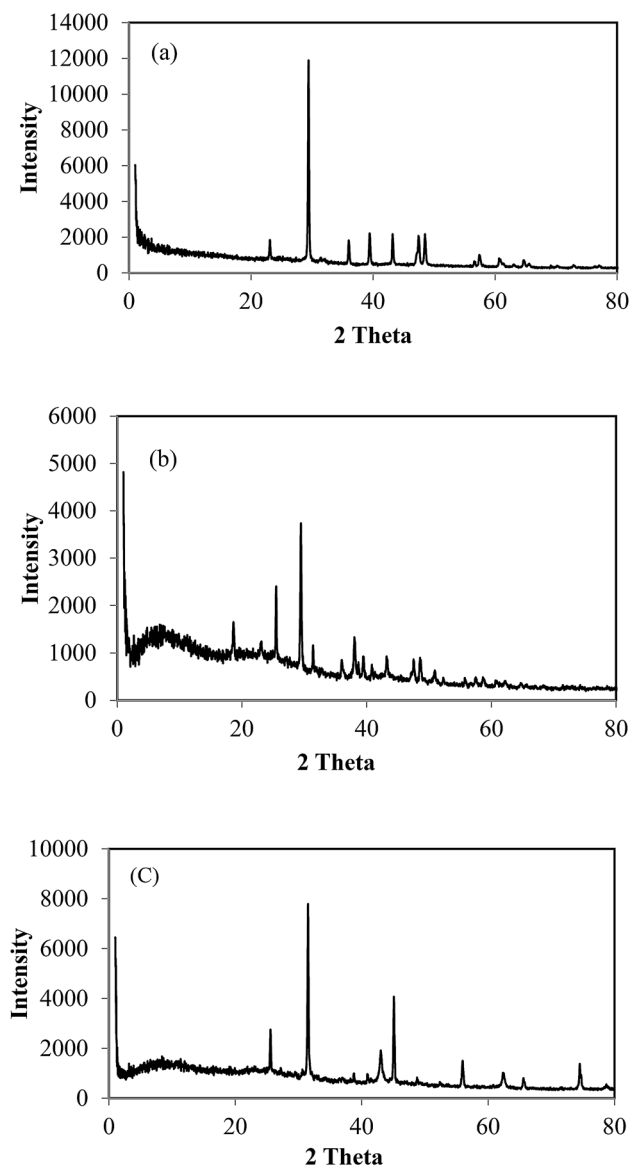


Fig. 3 XRD spectrum of activated carbon produced from *Citrus limon* tree leaves (a) before the adsorption, b after the adsorption of lead ions, and c after adsorption of arsenic ions

ions to locate on the adsorbent active sites. Therefore, the adsorbent's total surface charge becomes positive and barricades the adsorption of positive-charged metallic ions on the adsorbent's surface. In this study, there was a reduction in adsorption efficiencies of lead and arsenic ions after pH values of 7 and 9, respectively. The observed drops were due to the formation of complexes of the hydroxide ions (OH^-) present in the solution as well as the competition between them and the remained metallic ions for relocation on adsorbent active sites [27]. Therefore, in this current study, the optimum pH values for lead and arsenic ions were equal to 7 and 9, respectively.

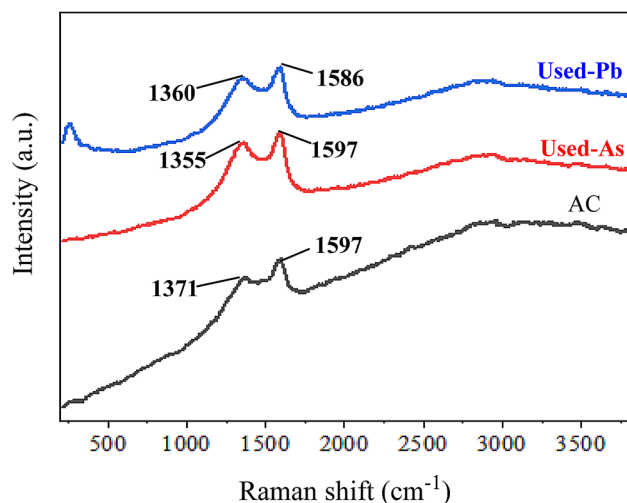


Fig. 4 Raman analysis for the prepared activated carbon from *Citrus limon* tree leaves before and after the adsorption of arsenic and lead ions from aqueous solution

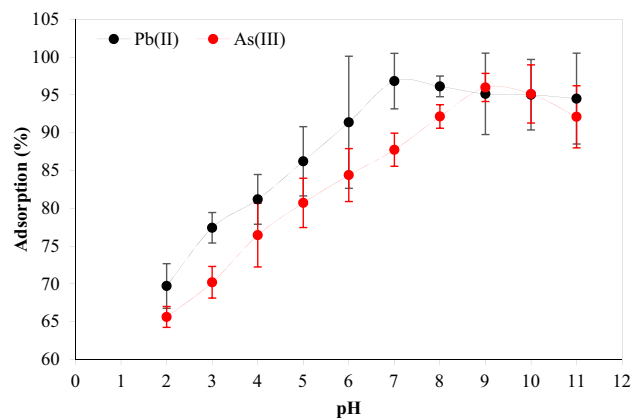


Fig. 5 The effect of solution pH on the adsorption efficiencies of lead and arsenic ions from the aqueous solution by the activated carbon prepared from *Citrus limon* tree leaves (adsorbent dosage = 0.25 g/L, Conc. = 20 mg/L, $T = 25^\circ\text{C}$, $t_c = 60$ min, and stirring rate = 200 rpm)

3.3 Effect of adsorbent dosage

Adsorbent dosage is one of the most important factors in adsorption process, because it helps achieving the maximum adsorption efficiency [28]. The effect of adsorbent dosage in the range of 0.25–10 g/L on the lead and arsenic adsorption efficiencies is shown in Fig. 6. As shown in this figure, by increasing the adsorbent dosage from 0.25 to 3 g/L, the removal percentages of lead and arsenic increased and then it became constant after the dosage of 3 g/L. As a result of increasing the adsorbent dosage, the specific surface area and number of active sites of the adsorbent increased which promote the adsorption of ions onto these sites which is

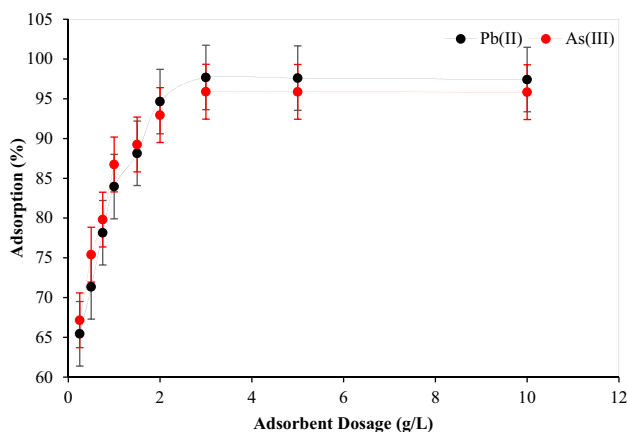


Fig. 6 The effect of adsorbent dosage on the adsorption efficiencies of lead and arsenic ions from the aqueous solution by the activated carbon prepared from *Citrus limon* tree leaves (pH=7 for lead and pH=9 for arsenic, Conc.=10 mg/L, $T=25\text{ }^{\circ}\text{C}$, $t_c=60\text{ min}$, and stirring rate=200 rpm)

followed by a rise in the adsorption efficiencies of lead and arsenic ions [29]. By the further increase in the adsorbent dosage, since a small amount of ions remained in the solution, there was a slight increase in the adsorption efficiency and after a while the process stopped finally. This phenomenon can be explained through the probability of aggregation of adsorbent particles because of their high mass which results in decrease of the adsorbent's surface area and increase of the diffusional path length [15]. As a result, the adsorbent dosage of 3 g/L was obtained as an optimum value, in which the removal efficiencies of lead and arsenic ions were 95.89% and 97.68%, respectively. These findings further support the idea that says the maximum adsorption occurs in an appropriate dosage of the adsorbent and no significant adsorption was found for the residual ions after this point.

3.4 Effect of ions initial concentration

The effect of initial concentration of lead and arsenic ions in the range of 10–100 mg/L on their removal efficiencies is shown in Fig. 7. As it can be observed, for the lower concentrations of the metallic ions, the removal percentages were high. The reason is that in the lower concentrations, the number of available active sites was higher for lead and arsenic ions, as a result, all of the ions can be easily adsorbed on the surface of adsorbent. By the further increase in the concentration of ions in the solution, the adsorption decreased, because of lack of adequate number of available active sites for the adsorption of ions. Thus, the highest removal efficiencies were obtained in the concentration of 10 mg/L for both of the ions. It should be noted that the maximum adsorption efficiencies of lead and arsenic ions

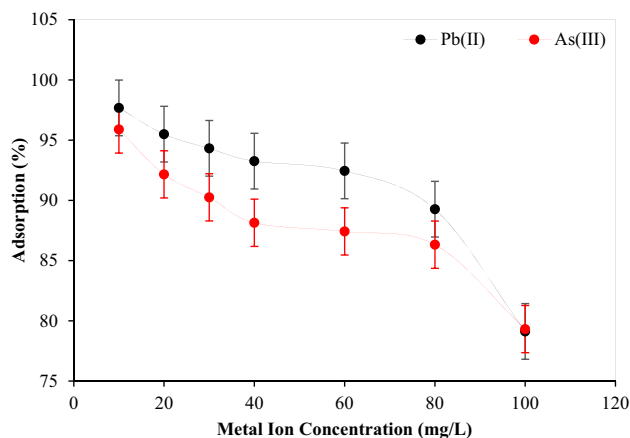


Fig. 7 The effect of arsenic and lead ions initial concentration on their adsorption efficiencies from the aqueous solution by the activated carbon prepared from *Citrus limon* tree leaves (pH=7 for lead and pH=9 for arsenic, adsorbent dosage=3 g/L, $T=25\text{ }^{\circ}\text{C}$, $t_c=60\text{ min}$, and stirring rate of 200 rpm)

in the achieved optimized ion concentration were of 97.68% and 95.89%, respectively.

3.5 Effects of contact time and temperature

Temperature is another important parameter of the adsorption, because it determines the exothermic/endothermic nature of the process. The effects of temperature and contact time on the removal efficiencies of lead and arsenic ions from aqueous solution by the activated carbon adsorbent in the range of 25–55 $^{\circ}\text{C}$ and 5–180 min are shown in Figs. 8 and 9, respectively. As shown in Fig. 8, there is an initial steep rise in adsorption efficiency which is the sign of high

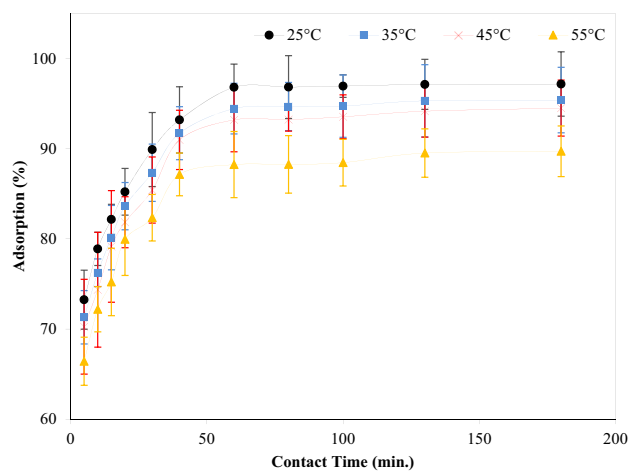


Fig. 8 The effect of temperature and contact time on the adsorption efficiency of lead ions from the aqueous solution by the activated carbon prepared from *Citrus limon* tree leaves (pH=7, Conc.=10 mg/L, adsorbent dosage=3 g/L, and stirring rate of 200 rpm)

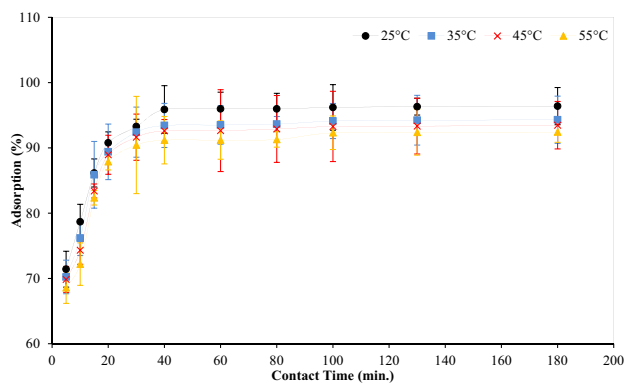


Fig. 9 The effect of temperature and contact time on the adsorption efficiency of arsenic ions from the aqueous solution by the activated carbon prepared from *Citrus limon* tree leaves (pH=9, Conc.=10 mg/L, adsorbent dosage=3 g/L and stirring rate of 200 rpm)

adsorption rates. This is due to the fact that at the beginning of the adsorption process, a large number of active sites are available for the metallic ions to be adsorbed, therefore the removal percentage is high. After 60 min, the slope of lead ion's adsorption curve decreased and then it gradually became constant. With increasing the contact time, due to gradual occupancy of these sites and repulsive forces between the ions and bulk of solution, the occupation of the remaining vacant sites becomes more difficult [30]. Therefore, this point, 60 min, can be the optimal value for the contact time of lead ions adsorption. From the data in Fig. 9, the contact time of 40 min was considered as the optimal value for removal of arsenic ions.

On the other hand, in Figs. 8 and 9 there is a clear trend of decreasing of adsorption efficiencies with temperature in the range of 25–55 °C for both of these ions. Based on these data, it can be concluded that the adsorption processes were more suitable in lower temperatures, which indicates that the current adsorption processes were exothermic and no chemical bonds were formed during the adsorption. Therefore, 25 °C was considered as the optimal temperature for both of ions. It is worth noting that the optimal adsorption efficiency of lead and arsenic ions were 97.68% and 95.89%, respectively.

3.6 Desorption and regeneration experiments

The complete mechanism of the adsorption process can be achieved through the desorption studies. In addition, regeneration of the adsorbent plays a key role in the economic success of the process [31]. In the current research, the desorption experiments of the prepared activated carbon after the adsorption of lead and arsenic ions were performed using NaOH solution (0.3 M) for different time periods and the results are presented in Fig. 10. As it can be seen, the two

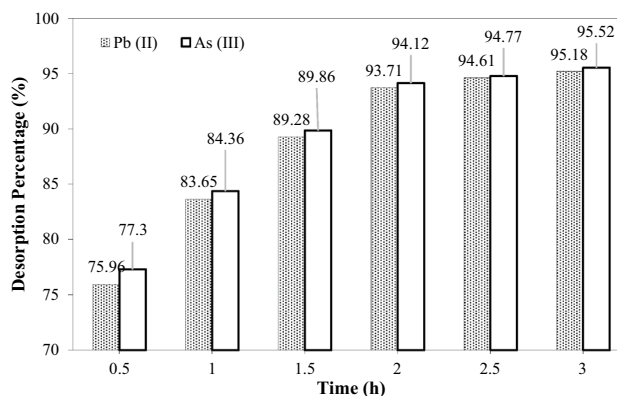


Fig. 10 The effect of contact time on the desorption efficiencies of lead and arsenic ions from the prepared activated carbon adsorbent

ions desorption percentage from the prepared adsorbent decreased with time. From the data it can be seen that the maximum desorption percentages for Pb and As ions were 93.71% (2 h) and 94.12% (2 h), respectively.

The results of reusing the adsorbent prepared from *Citrus limon* tree leaves for 6 stages of adsorption/desorption process is presented in Fig. 11. As it can be observed, there is a mild decline (6%) in the adsorption efficiencies of the prepared adsorbent in the first four stages of adsorption/desorption process. After this point, the decline in adsorption capacity was considerable, which can be related to the competition between OH^- and pollutant ions for sitting on the adsorbent's surface [32]. Therefore, the most striking result to emerge from these data is that the activated carbon adsorbent prepared from *Citrus limon* tree leaves can be used for four stages of adsorption/desorption of Pb and As ions from the aqueous solutions and can be considered as an appropriate one for the removal of these pollutants.

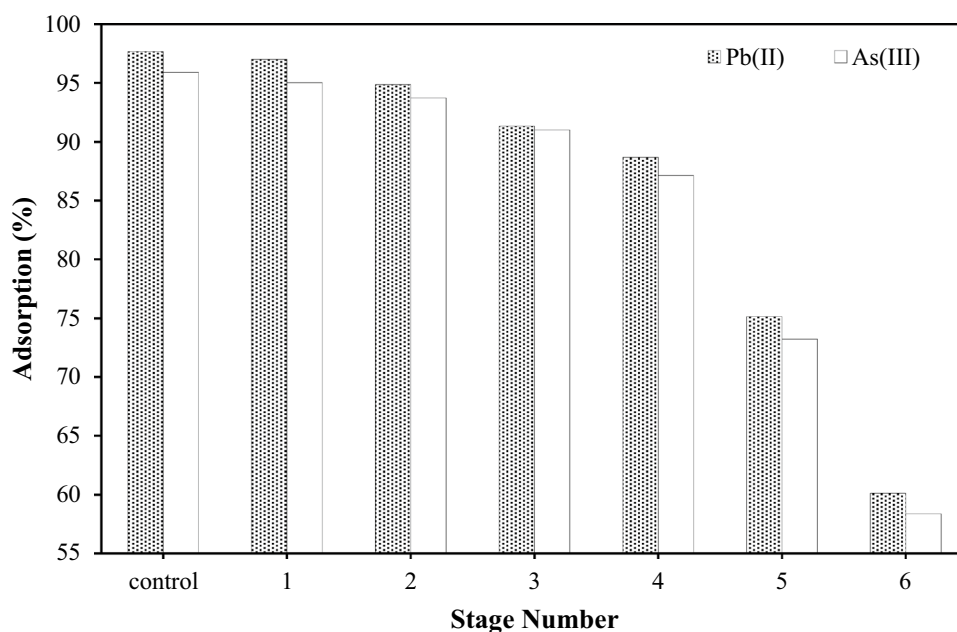
3.7 Adsorption isotherms

The adsorption isotherm represents valuable information about the ions and adsorbent interactions. To study the equilibrium behavior of the lead and arsenic adsorption processes, Langmuir and Freundlich isotherm models were applied. Langmuir isotherm is used to describe the single layer adsorption on surfaces with a finite number of adsorption sites. The linear form of the Langmuir equation is given by Eq. (3) [33, 34]:

$$\frac{C_e}{q_e} = \frac{1}{K_L q_m} + \frac{C_e}{q_m} \quad (3)$$

In this equation, q_{max} and K_L are the adsorption isotherm model constants which show the highest adsorption capacity (mg/g) and adsorption energy (L/mg), respectively. The

Fig. 11 Adsorption/desorption studies of lead and arsenic ions using the activated carbon adsorbent prepared from *Citrus limon* tree leaves



values of these two constants are obtained from the slope and intercept of C_e/q_e versus C_e plot. The most important feature of Langmuir isotherm is R_L , which is called the adsorption intensity parameter, and is calculated using Eq. (4):

$$R_L = \frac{1}{1 + K_L C_i} \quad (4)$$

If the value of this parameter is $0 < R_L < 1$, $R_L > 1$, $R_L = 1$, and $R_L = 0$, the process is favorable, unfavorable, linear, and irreversible, respectively [10].

Freundlich model is an experimental model based on adsorption on a heterogeneous surface. The linear form of this model is given in Eq. (5):

$$\ln q_e = \frac{1}{n} \ln C_e + \ln K_f, \quad (5)$$

where K_f (L/mg) and n are the Freundlich constants which indicate the adsorption rate and degree of nonlinearity of the process. If the value of n is one, the adsorption is linear. Additionally, when it is lower and higher than 1, the adsorption is unfavorable and favorable, respectively [35]. The values of K_f and $1/n$ are obtained from the slope and intercept of $\ln q_e$ versus $\ln C_e$ plot.

Figure 12 and Table 3 present the plots and parameters of Langmuir and Freundlich isotherm models obtained from the experimental data of lead and arsenic ions adsorption. According to the equilibrium study results, the values of R_L of Langmuir isotherm for lead and arsenic ions were 0.133 and 0.263, respectively, indicating that their adsorption processes were favorable. Furthermore, the maximum adsorption capacities which were obtained using Langmuir model

were 45.66 mg/g and 52.91 mg/g for lead and arsenic ions, respectively. These values denote that the prepared adsorbent has a considerable adsorption capability.

In addition, using Freundlich isotherm model, the value of the n coefficient for lead and arsenic ions were equal to 1.99 and 1.74, respectively. Based on these values, it can be said that the current adsorption processes were physical and favorable. Also, according to the correlation coefficient values given in Table 3, Langmuir and Freundlich isotherm models performed well for describing lead and arsenic ions adsorption, respectively.

3.8 Kinetic study

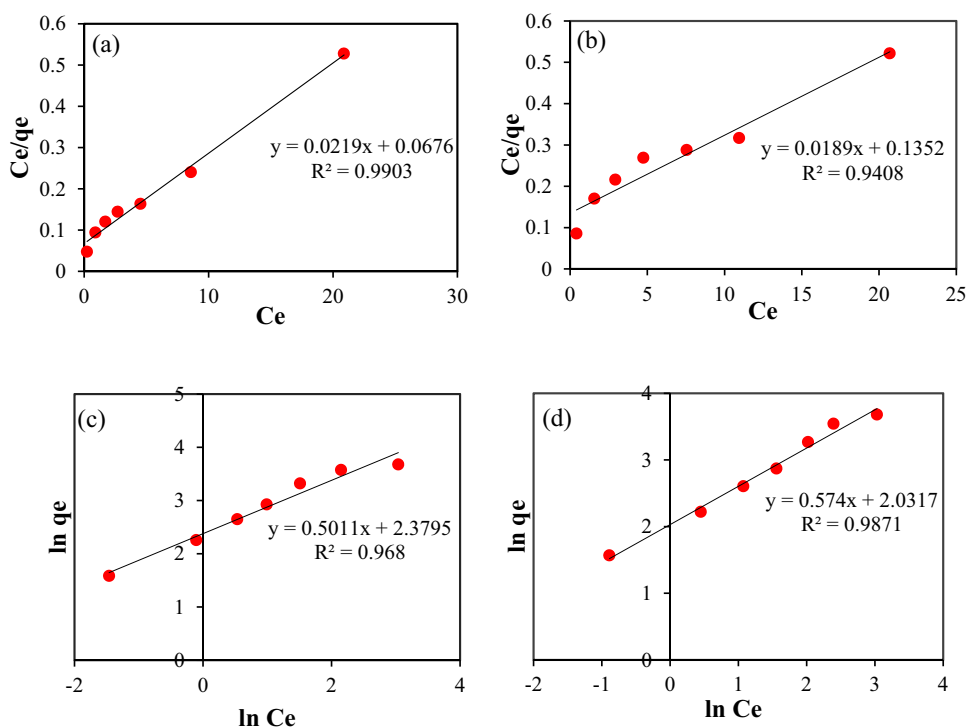
Adsorption process kinetics involves several steps such as transferring the pollutant to the adsorbent surface, transferring from the surface to the intermolecular active sites and remaining in the active sites through the adsorption, and complex formation or sedimentation [36]. The pseudo first-order and the pseudo second-order kinetic models were applied to study the kinetics of lead and arsenic removal from the aqueous solutions.

In the pseudo-first-order kinetic model, it is assumed that the adsorption rate is proportional to the number of adsorbent's active sites. The linear form of this model is expressed in Eq. (6) [37]:

$$\ln(q_e - q_t) = \ln q_e - K_1 t. \quad (6)$$

In this equation, q_t is the value of adsorbed ions at time t per gram of adsorbent (mg/g) and K_1 is the adsorption rate constant for the pseudo first-order model (1/min). K_1 and q_e

Fig. 12 Langmuir isotherm model diagrams for the adsorption of (a) lead and (b) arsenic ions and the Freundlich isotherm model diagrams for the adsorption of (c) lead and (d) arsenic ions from aqueous solution by activated carbon adsorbent prepared from *Citrus limon* tree leaves (pH=7 for lead and pH=9 for arsenic, adsorbent dosage = 3 g/L, $T=25\text{ }^{\circ}\text{C}$, $t_c=60\text{ min}$, and stirring rate = 200 rpm)



are calculated using the slope and intercept of $\ln(q_e - q_t)$ versus t plot [38].

The pseudo second-order kinetic model is based on the hypothesis that the occupation rate of active sites by the adsorbates is proportional to the squared of the number of unoccupied sites. The linear form of the pseudo second-order kinetic model is given by Eq. (7) [39, 40]:

$$\frac{t}{q_t} = \frac{1}{K_2 q_e^2} + \frac{t}{q_e}, \quad (7)$$

where K_2 is the pseudo second kinetic rate constant ($\text{g mg}^{-1} \text{g}^{-1}$). Additionally, the values of q_e and K_2 are determined from the slope and intercept of the t/q_t versus t [38, 39].

Table 3 Langmuir and Freundlich adsorption isotherm parameters for the adsorption of lead and arsenic ions by the activated carbon adsorbent prepared from *Citrus limon* tree leaves

Models	Parameters	Pb (II)	As (III)
Langmuir	q_m (mg/g)	45.66	52.91
	K_L (L/mg)	0.324	0.139
	R^2	0.9903	0.968
	R_L	0.133	0.263
Freundlich	n	1.99	1.74
	K_f (mg/g (L/mg) ^{1/n})	10.97	7.667
	R^2	0.968	0.9871

The results of kinetic study for the adsorption of lead and arsenic ions are shown in Fig. 13. In addition, the values of the calculated parameters are presented in Tables 4. According to the achieved results, the experimental values of the adsorbed ions at equilibrium time for both of metal ions ($q_{e,\text{exp}}$) were the highest in $25\text{ }^{\circ}\text{C}$. Additionally, considering the R^2 values for the proposed models, it can be concluded that the pseudo second-order kinetic model performed better than that of pseudo first-order model for the description of the kinetic behavior of lead and arsenic ions adsorption using the activated carbon prepared from *Citrus limon* tree leaves.

3.9 Thermodynamic study

Using the thermodynamic parameters, one can describe the nature of the reaction (exothermic or endothermic). In thermodynamic studies, the parameters such as enthalpy (ΔH°), entropy (ΔS°), and Gibbs free energy (ΔG°) are calculated. The adsorption equilibrium constant (K_e) is calculated using Eq. (8) [39]:

$$K_e = \frac{q_e}{C_e}. \quad (8)$$

The value of K_e is used to calculate the Gibbs free energy as follows:

$$\Delta G^\circ = -RT \ln K_e. \quad (9)$$

Fig. 13 Pseudo-first-order kinetic model diagrams for the adsorption of (a) lead and (b) arsenic ions and pseudo second-order kinetic model diagrams for the adsorption of (c) lead and (d) arsenic ions from aqueous solution by activated carbon adsorbent prepared from *Citrus limon* tree leaves

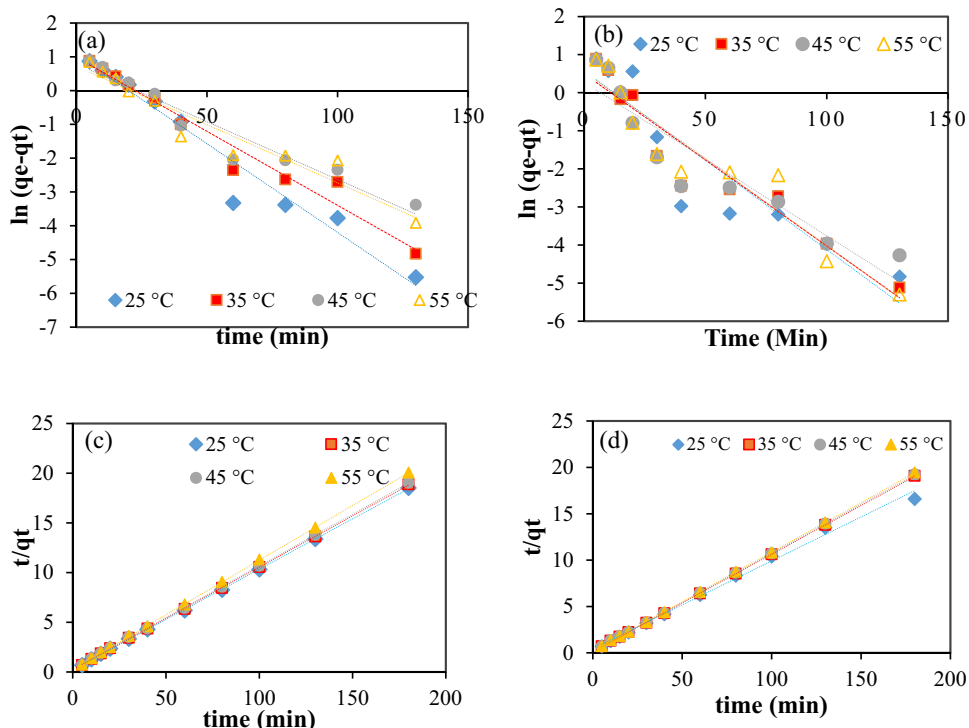


Table 4 Pseudo first-order and pseudo second-order kinetic parameters for the adsorption of lead and arsenic metal ions by the activated carbon adsorbent prepared from *Citrus limon* tree leaves

Kinetic models	Parameters	25 °C	35 °C	45 °C	55 °C	
Pb (II)	Pseudo first-order	$q_{e,cal}$	2.87	2.672	2.207	2.046
		K_1	0.0525	0.0438	0.0342	0.0345
		R^2	0.9586	0.9652	0.9419	0.9308
	Pseudo second-order	K_2	0.0422	0.0401	0.0376	0.0438
		$q_{e,cal}$	9.891	9.708	9.615	9.107
		R^2	0.9999	0.9999	0.9999	0.9999
	$q_{e,exp}$	0.718	9.54	9.451	8.972	
AS (III)	Pseudo first-order	$q_{e,cal}$	1.7785	1.6437	1.3144	1.7446
		K_1	0.0469	0.0452	0.0403	0.0485
		R^2	0.868	0.9151	0.871	0.9137
	Pseudo second order	K_2	0.058	0.067	0.068	0.062
		$q_{e,cal}$	10.548	9.532	9.451	9.3545
		R^2	0.9937	0.9999	0.9999	0.9999
		$q_{e,exp}$	9.64	9.431	9.348	9.254

In Eq. (9), ΔG° is the Gibbs free energy (J/mol), R is the universal gas constant (8.314 J/mol K), and T is the absolute temperature (Kelvin).

The equilibrium constant can be expressed as a function of temperature, enthalpy (ΔH°), and entropy (ΔS°)

Table 5 Thermodynamic parameters of the adsorption processes of lead and arsenic metal ions from the aqueous solution by the activated carbon adsorbent prepared from *Citrus limon* tree leaves

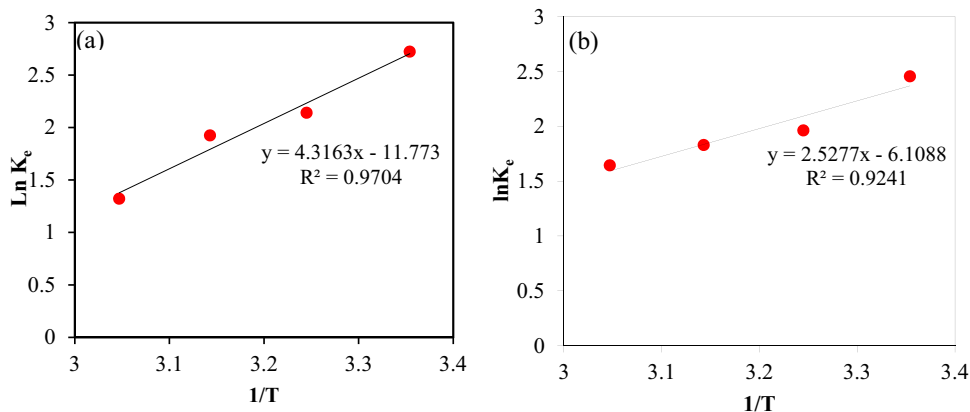
Metal ions	T (°C)	ΔG° (kJ/mol)	ΔH° (kJ/mol)	ΔS° (J/mol K)
Pb (II)	25	-6.7454	-35.88	-97.88
	35	-5.47		
	45	-5.089		
	55	-3.602		
As (II)	25	-6.058	-21.01	-50.78
	35	-5.018		
	45	-4.7		
	55	-4.47		

variations. The relationship between K_e and temperature is presented by Van't Hoff's equation, which is expressed as follows [41]:

$$\ln K_e = -\frac{\Delta H^\circ}{RT} + \frac{\Delta S^\circ}{R} \tag{10}$$

Using the slope and intercept values of $\ln K_e$ versus $1/T$ line, ΔH° and ΔS° of the adsorption process are calculated [42]. Table 5 shows the values of thermodynamic parameters at different temperatures. Figure 14 is also illustrated to display the adsorption thermodynamics of lead and arsenic ions by the adsorbent prepared from *Citrus limon* tree leaves at different temperatures.

Fig. 14 Thermodynamic diagrams of the adsorption process of (a) lead and (b) arsenic ions from aqueous solution by activated carbon adsorbent prepared from *Citrus limon* tree leaves (pH=7 for lead and pH=9 for arsenic, adsorbent dosage = 3 g/L, Conc. = 10 mg/L, and $t_c = 60$ min)



According to the findings presented in Table 5, Gibbs free energy (ΔG°) in 25 °C for lead and arsenic ions were -6.7454 kJ/mol and -6.085 kJ/mol, respectively, which denote that the adsorption processes of these ions by the adsorbent prepared from *Citrus limon* tree leaves were possible and spontaneous. Additionally, there was a negative correlation between Gibbs free energy and temperature, therefore it is possible to adsorb the ions in higher temperatures. Also, the enthalpy changes in the temperature range of 25–55 °C were -35.88 J/mol and -21.01 J/mol for lead and arsenic ions, respectively. Consequently, the adsorption processes of both of these ions were exothermic. In addition, the negative values of entropy change (ΔS°) indicates that the adsorption processes of these ions were reversible and physical.

4 Conclusion

In this study, adsorption of lead and arsenic ions from aqueous solutions using the activated carbon prepared from *Citrus limon* tree leaves was investigated. The results showed that the optimum pH and contact time were 7 and 60 min for lead and 9 and 40 min for arsenic ions, while the temperature of 25 °C, ion concentration of 10 mg/L, and adsorbent dosage of 3 g/L were the best conditions for both of them. In addition, the current adsorbent showed an acceptable adsorption capability after four stages of adsorption/desorption processes of the mentioned ions. Adsorption equilibrium studies revealed that Langmuir and Freundlich models were appropriate for describing the adsorption equilibrium behavior of lead and arsenic ions, respectively. Kinetic studies showed that the pseudo second-order kinetic model performed well for describing the removal process mechanism of lead and arsenic ions. Additionally, the negative values of Gibbs free energy showed that the processes were spontaneous for both of the metal ions.

References

- Paul J, Rawat K, Sarma K, Sabharwal S (2011) Decoloration and degradation of reactive red-120 dye by electron beam irradiation in aqueous solution. *Appl Radiat Isot* 69(7):982–987
- Bulgariu L, Bulgariu D, Macoveanu M (2011) Adsorptive performances of alkaline treated peat for heavy metal removal. *Sep Sci Technol* 46(6):1023–1033
- Nacu G, Negri L, Bulgariu L (2017) Batch adsorption of Zn (II) ions from aqueous solution onto sawdust. *Rev Roum Chim* 62(4–5):439–447
- Fu F, Wang Q (2011) Removal of heavy metal ions from wastewaters: a review. *J Environ Manage* 92(3):407–418
- Mousavi SM, Hashemi SA, Amani AM, Esmaeili H, Ghasemi Y, Babapoor A, Mojoudi F, Arjomand O (2018) Pb (II) removal from synthetic wastewater using kombucha scoby and graphene oxide/ Fe_3O_4 . *Phys Chem Res* 6(4):759–771
- Saman N, Johari K, Song S-T, Kong H, Cheu S-C, Mat H (2016) High removal efficiency of Hg (II) and MeHg (II) from aqueous solution by coconut pith—equilibrium, kinetic and mechanism analyses. *J environmental chemical engineering* 4(2):2487–2499
- Bhatnagar A, Sillanpää M (2010) Utilization of agro-industrial and municipal waste materials as potential adsorbents for water treatment—a review. *Chem Eng J* 157(2–3):277–296
- Hashim MA, Mukhopadhyay S, Sahu JN, Sengupta B (2011) Remediation technologies for heavy metal contaminated groundwater. *J Environ Manage* 92(10):2355–2388
- Volf I, Rakoto NG, Bulgariu L (2015) Valorization of *Pistia stratiotes* biomass as biosorbent for lead (II) ions removal from aqueous media. *Sep Sci Technol* 50(10):1577–1586
- Foroutan R, Mohammadi R, Farjadfar S, Esmaeili H, Saberi M, Sahebi S, Dobaradaran S, Ramavandi B (2019) Characteristics and performance of Cd, Ni, and Pb bio-adsorption using *Callinectes sapidus* biomass: real wastewater treatment. *Environ Sci Pollut Res* 26(7):6336–6347
- Mousavi SM, Hashemi SA, Esmaeili H, Amani AM, Mojoudi F (2018) Synthesis of Fe_3O_4 nanoparticles modified by oak shell for treatment of wastewater containing Ni (II). *Acta Chim Slov* 65(3):750–756
- Baral S, Das N, Chaudhury GR, Das S (2009) A preliminary study on the adsorptive removal of Cr (VI) using seaweed, *Hydrilla verticillata*. *J Hazard Mater* 171(1–3):358–369
- Ramavandi B, Farjadfar S (2014) Removal of chemical oxygen demand from textile wastewater using a natural coagulant. *Korean J Chem Eng* 31(1):81–87
- Harja M, Buema G, Bulgariu L, Bulgariu D, Sutiman DM, Ciobanu G (2015) Removal of cadmium (II) from aqueous

- solution by adsorption onto modified algae and ash. *Korean J Chem Eng* 32(9):1804–1811
15. Royer B, Cardoso NF, Lima EC, Vaghetti JC, Simon NM, Calvete T, Veses RC (2009) Applications of Brazilian pine-fruit shell in natural and carbonized forms as adsorbents to removal of methylene blue from aqueous solutions—kinetic and equilibrium study. *J Hazard Mater* 164(2–3):1213–1222
 16. Nacu G, Bulgariu D, Cristina Popescu M, Harja M, Toader Juravle D, Bulgariu L (2016) Removal of Zn (II) ions from aqueous media on thermal activated sawdust. *Desalination Water Treat* 57(46):21904–21915
 17. Abshirini Y, Foroutan R, Esmaeili H (2018) Cr (VI) removal from aqueous solution using activated carbon prepared from *Ziziphus spina-christi* leaf. *Mat Res Exp* 6:045607
 18. Khademi Z, Ramavandi B, Ghaneian MT (2015) The behaviors and characteristics of a mesoporous activated carbon prepared from *Tamarix hispida* for Zn (II) adsorption from wastewater. *J Environ Chem Eng* 3(3):2057–2067
 19. Esmaeili H, Foroutan R (2019) Adsorptive behavior of methylene blue onto sawdust of sour lemon, date palm, and eucalyptus as agricultural wastes. *J Dispersion Sci Technol* 40(7):990–999
 20. Yao S, Zhang J, Shen D, Xiao R, Gu S, Zhao M, Liang J (2016) Removal of Pb (II) from water by the activated carbon modified by nitric acid under microwave heating. *J Colloid Interface Sci* 463:118–127
 21. Wang K, Zhao J, Li H, Zhang X, Shi H (2016) Removal of cadmium (II) from aqueous solution by granular activated carbon supported magnesium hydroxide. *J Taiwan Inst Chem Eng* 61:287–291
 22. Saleh TA, Alhooshani KR, Abdelbassit MS (2015) Evaluation of AC/ZnO composite for sorption of dichloromethane, trichloromethane and carbon tetrachloride: kinetics and isotherms. *J Taiwan Inst Chem Eng* 55:159–169
 23. Hayati B, Maleki A, Najafi F, Gharibi F, McKay G, Gupta VK, Puttaiah SH, Marzban N (2018) Heavy metal adsorption using PAMAM/CNT nanocomposite from aqueous solution in batch and continuous fixed bed systems. *Chem Eng J* 346:258–270
 24. Shi T, Jia S, Chen Y, Wen Y, Du C, Guo H, Wang Z (2009) Adsorption of Pb (II), Cr (III), Cu (II), Cd (II) and Ni (II) onto a vanadium mine tailing from aqueous solution. *J Hazard Mater* 169(1–3):838–846
 25. Dong C, Lu J, Qiu B, Shen B, Xing M, Zhang J (2018) Developing stretchable and graphene-oxide-based hydrogel for the removal of organic pollutants and metal ions. *Appl Catal B* 222:146–156
 26. Klekotka U, Wińska E, Zambrzycka-Szelewa E, Satuła D, Kalska-Szostko B (2018) Heavy-metal detectors based on modified ferrite nanoparticles. *Beilstein J Nanotechnol* 9(1):762–770
 27. Lawal O, Sanni A, Ajayi I, Rabiu O (2010) Equilibrium, thermodynamic and kinetic studies for the biosorption of aqueous lead (II) ions onto the seed husk of *Calophyllum inophyllum*. *J Hazard Mater* 177(1–3):829–835
 28. Ahmad A, Rafatullah M, Sulaiman O, Ibrahim MH, Chii YY, Siddique BM (2009) Removal of Cu (II) and Pb (II) ions from aqueous solutions by adsorption on sawdust of Meranti wood. *Desalination* 247(1–3):636–646
 29. Shirmardi M, Alavi N, Lima EC, Takdastan A, Mahvi AH, Babaei AA (2016) Removal of atrazine as an organic micro-pollutant from aqueous solutions: a comparative study. *Process Saf Environ Prot* 103:23–35
 30. Takdastan A, Mahvi AH, Lima EC, Shirmardi M, Babaei AA, Goudarzi G, Neisi A, Heidari Farsani M, Vosoughi M (2016) Preparation, characterization, and application of activated carbon from low-cost material for the adsorption of tetracycline antibiotic from aqueous solutions. *Water Sci Technol* 74(10):2349–2363
 31. Dehghani MH, Dehghan A, Alidadi H, Dolatabadi M, Mehrabpour M, Converti A (2017) Removal of methylene blue dye from aqueous solutions by a new chitosan/zeolite composite from shrimp waste: kinetic and equilibrium study. *Korean J Chem Eng* 34(6):1699–1707
 32. Kumar IA, Viswanathan N (2018) Preparation and testing of a tetra-amine copper (II) chitosan bead system for enhanced phosphate remediation. *Carbohydr Polym* 183:173–182
 33. Chiou M-S, Li H-Y (2002) Equilibrium and kinetic modeling of adsorption of reactive dye on cross-linked chitosan beads. *J Hazard Mater* 93(2):233–248
 34. Febrianto J, Kosasih AN, Sunarjo J, Ju Y-H, Indraswati N, Ismadji S (2009) Equilibrium and kinetic studies in adsorption of heavy metals using biosorbent: a summary of recent studies. *J Hazard Mater* 162(2–3):616–645
 35. Fang F, Kong L, Huang J, Wu S, Zhang K, Wang X, Sun B, Jin Z, Wang J, Huang X-J (2014) Removal of cobalt ions from aqueous solution by an amination graphene oxide nanocomposite. *J Hazard Mater* 270:1–10
 36. Lima EC, Royer B, Vaghetti JC, Simon NM, da Cunha BM, Pavan FA, Benvenuti EV, Cataluña-Veses R, Airolidi C (2008) Application of Brazilian pine-fruit shell as a biosorbent to removal of reactive red 194 textile dye from aqueous solution: kinetics and equilibrium study. *J Hazard Mater* 155(3):536–550
 37. Wang P, Du M, Zhu H, Bao S, Yang T, Zou M (2015) Structure regulation of silica nanotubes and their adsorption behaviors for heavy metal ions: pH effect, kinetics, isotherms and mechanism. *J Hazard Mater* 286:533–544
 38. Mousavi M, Hashemi A, Arjmand O, Amani AM, Babapoor A, Fateh MA, Fateh H, Mojoudi F, Esmaeili H, Jahandideh S (2018) Erythrosine adsorption from aqueous solution via decorated graphene oxide with magnetic iron oxide nano particles: kinetic and equilibrium studies. *Acta Chim Slov* 65(4):882–894
 39. Liu F, Li L, Ling P, Jing X, Li C, Li A, You X (2011) Interaction mechanism of aqueous heavy metals onto a newly synthesized IDA-chelating resin: isotherms, thermodynamics and kinetics. *Chem Eng J* 173(1):106–114
 40. Matouq M, Jildeh N, Qtaishat M, Hindiyeh M, Al Syouf MQ (2015) The adsorption kinetics and modeling for heavy metals removal from wastewater by *Moringa pods*. *J Environ Chem Eng* 3(2):775–784
 41. Nashine A, Tembhurkar A (2016) Equilibrium, kinetic and thermodynamic studies for adsorption of As (III) on coconut (*Cocos nucifera* L.) fiber. *J Environ Chem Eng* 4(3):3267–3273
 42. Aksu Z, İsoğlu İA (2005) Removal of copper (II) ions from aqueous solution by biosorption onto agricultural waste sugar beet pulp. *Process Biochem* 40(9):3031–3044